pers at core.ac.uk

Open Archive Toulouse Archive Ouverte (OATAO)
OATAO is an open access repository that collects the work of Toulouse researchers and makes it freely available over the web where possible.

This is an author -deposited version published in: http://oatao.univ-toulouse.fr/
Eprints ID: 4893

To link to this article: DOI:10.1016/j.crme.2011.03.014

http://dx.doi.org/10.1016/j.crme.2011.03.014

To cite this version : Davarzani, Hossein and Marcoux, Manuel *Influence of solid phase thermal conductivity on species separation rate in packed thermogravitational columns: A direct numerical simulation model.* (2011) Comptes Rendus Mécanique, vol. 339 (n° 5). pp. 355-361. ISSN 1631-0721

Any correspondence concerning this service should be sent to the repository administrator: staff-oatao@inp-toulouse.fr

Thermodiffusion and coupled phenomena / Thermodiffusion et phénomènes couplés

Influence of solid phase thermal conductivity on species separation rate in packed thermogravitational columns: A direct numerical simulation model

Hossein Davarzani, Manuel Marcoux *

Université de Toulouse; INPT, UPS; IMFT (Institut de Mécanique des Fluides de Toulouse), Groupe d'Étude sur les Milieux Poreux, allée du Professeur Camille Soula, 31400 Toulouse, France

Keywords:
Thermogravitational cell
Thermal conductivity
Soret effect
Porous media
Binary mixture
Separation

A B S T R A C T

In this work, a direct numerical simulation model has been proposed to study the influence of porous matrix thermal properties on the separation rate in a model of packed thermogravitational column saturated by a binary mixture.
The coupled flow, heat and mass dimensionless equations and boundary conditions have been derived in pore-scale and then solved over a vertical column containing fluid and solid phases.
The results show that the separation rate is changed significantly by the conductivity ratio of the solid/fluid phases. The classical maximum separation at optimal Rayleigh number increases by decreasing the solid thermal conductivity. We obtained that the influence of the solid thermal conductivity for small Rayleigh number is not considerable but for intermediate Rayleigh number the separation rate initially decreases with increasing the thermal conductivity ratio and then reaches an asymptote. As the Rayleigh number increases, convection dominates and the effect of thermal conductivity ratio on separation rate becomes completely inversed.

1. Introduction

It is now well known, since the early works of Clusius and Dickel (1939) [1], Furry et al. (1939) [2], and De Groot (1942) [3] that, the coupling of a fluid mixture circulation due to convection with the phenomenon of thermodiffusion amplifies the elementary separation coming from the Soret effect. This phenomenon which creates a concentration difference between top and bottom of the column is known as the thermogravitational effect, and is used in the thermodiffusion cells with the same name to separate species and to determine the Soret coefficient of the mixture with more precision [4,5].

However, the optimal conditions of coupling between the vertical advective transport and thermodiffusion generally correspond to very thin cavity, with a gap of less than one millimeter [6,7]. Some authors have had the idea of filling the thermogravitational cells with a porous medium [8]. This allows replacing of the thin cavity gap constraint in free fluid with the pore spacing of porous medium. In such a packed thermogravitational cell, the maximum separation is associated to an optimal permeability of porous medium which is also more easily accessible experimentally [9,10]. This also allows study of the multicomponent transport subjected to thermal gradients in geological conditions, such as the study of compositional variation in hydrocarbon reservoirs [11].

* Corresponding author.
E-mail address: marcoux@imft.fr (M. Marcoux).

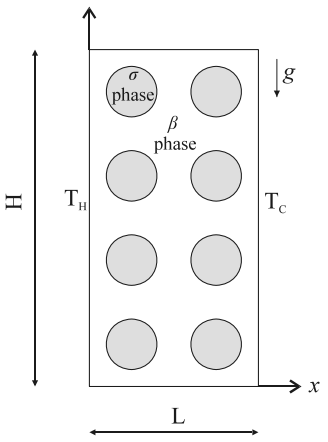

Fig. 1. Problem configuration ($\varepsilon_\beta = 0.8$).

The separation in a thermogravitational column can be also increased by inclining the column [12]. Recently, Mojtabi et al. (2003) showed that the vibrations can lead whether to increase or to decrease heat and mass transfers or delay or accelerate the onset of convection [13]. The study of the monocellular flow appearing at the onset of the convection in a horizontal porous cavity saturated by a binary mixture and heated from below showed that the optimal Rayleigh number in the horizontal cell is larger than that of the vertical one [14].

While the transfer of species related to thermodiffusion in porous media may directly be linked to the physical and thermal properties of the solid structures, various theoretical studies had generally treated this problem considering the whole system as an equivalent continuum (macroscopic approach) [15,16].

Some recent works have investigated the influence of the physical and thermal properties of the porous matrix on thermodiffusion by using upscaling technique [17,18]. At the upscaled model, the description of the flow of phases introduces new equations with the effective properties. These effective properties can be theoretically deduced from microscopic properties. These studies have shown that when the fluid crosses the medium with a low filtration velocity compared to diffusion (small Péclet number), the thermodiffusion coefficient in porous media is confirmed to be derived directly from the one in free medium by dividing it by the tortuosity coefficient of the medium. In the opposite, when convection is dominating, the Soret number in porous media is not equal to the one in free medium. At this regime, thermal properties of the porous medium have an important influence on the effective thermodiffusion coefficients [17]. In their model, the effective thermodiffusion coefficient in porous media decreases with increasing the forced convection; whereas, we know that in a thermogravitational cell, increasing convection causes increasing the separation up to a maximum rate.

This study aims to address this point by direct numerical simulation, treating all the dynamics, thermal and solutal transfers occurring at pore scale in a thermogravitational column in porous media with a solid phase made of arrays of cylinders.

The governing pore scale equations are derived in Section 2. Next, the equations are solved numerically over the thermogravitational cell and the parametric results are discussed in Section 3.

2. Mathematical formulation

We consider in this study a cavity of height H and length L (aspect ratio $A = H/L$) saturated with a binary mixture fluid and subjected to a horizontal thermal gradient. This system is illustrated in Fig. 1; the fluid phase is identified as the β-phase while the rigid, solid phase is represented by the σ-phase. The vertical walls are maintained at constant and different temperatures T_H and T_C whereas the horizontal walls are adiabatic.

The total mass density variation, in the β-phase, with temperature and mass fraction is described by the Boussinesq approximation for fluid phase:

$$\rho_\beta = \rho_0\big[1 - \beta_T(T_\beta - T_0) - \beta_C(c_\beta - c_0)\big], \quad \text{in the } \beta\text{-phase} \tag{1}$$

where T_β and c_β are the temperature and the mass fraction in the β-phase, ρ_0 is the fluid mixture density at temperature T_0 and mass fraction c_0. β_T and β_C are the thermal and solutal expansion coefficients, respectively.

The equations of continuity and motion have to be introduced for the fluid phase. We use Stokes equation for the flow motion at the pore-scale, assuming usually negligible inertia effects in porous media. The continuity equation, the Stokes equation, and the no-slip boundary condition are then written as:

$$\nabla.\mathbf{v}_\beta = 0, \quad \text{in the } \beta\text{-phase} \tag{2}$$

$$0 = -\nabla p_\beta + \mu_\beta \nabla.(\nabla \mathbf{v}_\beta) + \rho_\beta \mathbf{g}, \quad \text{in the } \beta\text{-phase} \tag{3}$$

$$\mathbf{v}_\beta = 0, \quad \text{at } \mathcal{A}_{\beta\sigma} \text{ and no-slip condition at all cavity boundary} \tag{4}$$

where $\mathbf{v}_\beta$ and p_β are the mass average velocity and the pressure in the β-phase, μ_β is the dynamic viscosity for the β-phase, $\mathbf{g}$ is the gravitational acceleration, $\mathcal{A}_{\beta\sigma}$ corresponds to the interface between the fluid phase and the solid phase and finally, $\mathbf{n}_{\beta\sigma}$ is the unit normal vector pointing from the fluid to the solid phase.

In this problem, we also consider the flow of the β-phase to be incompressible. We neglect the Dufour effect, which is justified in the case of liquids. Therefore, the pore-scale transport of energy is described by the following equations and boundary conditions for the fluid (conduction and convection) and solid (conduction) phases with continuity boundary condition on the surface of the β–σ interface ($\mathcal{A}_{\beta\sigma}$):

$$(\rho c_p)_\beta \frac{\partial T_\beta}{\partial t} + (\rho c_p)_\beta \nabla.(T_\beta \mathbf{v}_\beta) = \nabla.(k_\beta \nabla T_\beta), \quad \text{in the } \beta\text{-phase} \tag{5}$$

$$(\rho c_p)_\sigma \frac{\partial T_\sigma}{\partial t} = \nabla.(k_\sigma \nabla T_\sigma), \quad \text{in the } \sigma\text{-phase} \tag{6}$$

$$T_\beta = T_\sigma, \quad \text{at } \mathcal{A}_{\beta\sigma} \tag{7}$$

$$\mathbf{n}_{\beta\sigma}.(k_\beta \nabla T_\beta) = \mathbf{n}_{\beta\sigma}.(k_\sigma \nabla T_\sigma), \quad \text{at } \mathcal{A}_{\beta\sigma} \tag{8}$$

$$T_\beta|_{x=0} = T_H \quad \text{and} \quad T_\beta|_{x=L} = T_C \tag{9}$$

$$\mathbf{n}_{\beta\sigma}.(k_\beta \nabla T_\beta) = 0, \quad \text{at } z = 0, H \tag{10}$$

where c_p is the heat capacity, x and z are the Cartesian coordinates, t is the time, k_β and k_σ are the thermal conductivity of the fluid and solid phases, and T_σ is the temperature of the σ-phase.

The component pore-scale mass transport (diffusion, thermodiffusion and advection) is described by the following equation for the fluid phase:

$$\frac{\partial c_\beta}{\partial t} + \nabla.(c_\beta \mathbf{v}_\beta) = \nabla.(D_\beta \nabla c_\beta + D_{T\beta} \nabla T_\beta), \quad \text{in the } \beta\text{-phase} \tag{11}$$

$$\mathbf{n}_{\beta\sigma}.(D_\beta \nabla c_\beta + D_{T\beta} \nabla T_\beta) = 0, \quad \text{at } \mathcal{A}_{\beta\sigma} \tag{12}$$

for an impervious boundary on the interface, where c_β is the mass fraction of one of the two components in the β-phase, D_β and $D_{T\beta}$ are the molecular isothermal diffusion coefficient and thermodiffusion coefficient. We neglect any accumulation and reaction of solute at the fluid–solid interface as well as the phenomenon of surface diffusion and sorption.

For such problems, the dimensionless analysis concerns microscopic equations governed by defining following dimensionless quantities: H (the cavity height) for length, $k_\beta/[H(\rho c)_\beta]$ for velocity, $H^2(\rho c)_\beta/k_\beta$ for time, $\rho_0 k_\beta^2/[H^2(\rho c)_\beta^2]$ for pressure, $\Delta T = T_H - T_C$ for temperature, and $\Delta c = \Delta T D_{T\beta}/D_\beta$ for mass fraction.

Then, the equations and boundary condition governing the continuity and conservation of momentum in dimensionless form are:

$$\nabla.\mathbf{v}'_\beta = 0, \quad \text{in the } \beta\text{-phase} \tag{13}$$

$$0 = -\nabla p'_\beta + Pr \nabla.(\nabla \mathbf{v}'_\beta) + Ra\, Pr\left(T'_\beta + \psi c'_\beta\right), \quad \text{in the } \beta\text{-phase} \tag{14}$$

$$\mathbf{v}'_\beta = 0, \quad \text{at } \mathcal{A}_{\beta\sigma} \text{ and no-slip condition at all cavity boundary} \tag{15}$$

The dimensionless energy equations and boundary conditions are:

$$\frac{\partial T'_\beta}{\partial t'} + \nabla.(T'_\beta \mathbf{v}'_\beta) = \nabla.(\nabla T'_\beta), \quad \text{in the } \beta\text{-phase} \tag{16}$$

$$\frac{\partial T'_\sigma}{\partial t'} = \nabla.(\kappa r_{\rho c_p} \nabla T'_\sigma), \quad \text{in the } \sigma\text{-phase} \tag{17}$$

$$T'_\beta = T'_\sigma, \quad \text{at } \mathcal{A}_{\beta\sigma} \tag{18}$$

$$\mathbf{n}_{\beta\sigma}.(\nabla T'_\beta) = \mathbf{n}_{\beta\sigma}.(\kappa \nabla T'_\sigma), \quad \text{at } \mathcal{A}_{\beta\sigma} \tag{19}$$

$$\mathbf{n}.(\nabla T'_\beta) = 0, \quad \text{at } z' = 0, 2 \tag{20}$$

$$T'_\beta|_{x'=0} = 1 \quad \text{and} \quad T'_\beta|_{x'=1} = 0 \tag{21}$$

and finally, the dimensionless form of species transport is:

$$\frac{\partial c'_\beta}{\partial t'} + \nabla.\left(c'_\beta \mathbf{v}'_\beta\right) = \frac{1}{Le} \nabla.(\nabla c'_\beta + \nabla T'_\beta), \quad \text{in the } \beta\text{-phase} \tag{22}$$

$$\mathbf{n}_{\beta\sigma}.(\nabla c'_\beta + \nabla T'_\beta) = 0, \quad \text{at } \mathcal{A}_{\beta\sigma} \tag{23}$$

$$\mathbf{n}.(\nabla c'_\beta + \nabla T'_\beta) = 0, \quad \text{at cavity walls} \tag{24}$$

The problem depends on six dimensionless numbers.

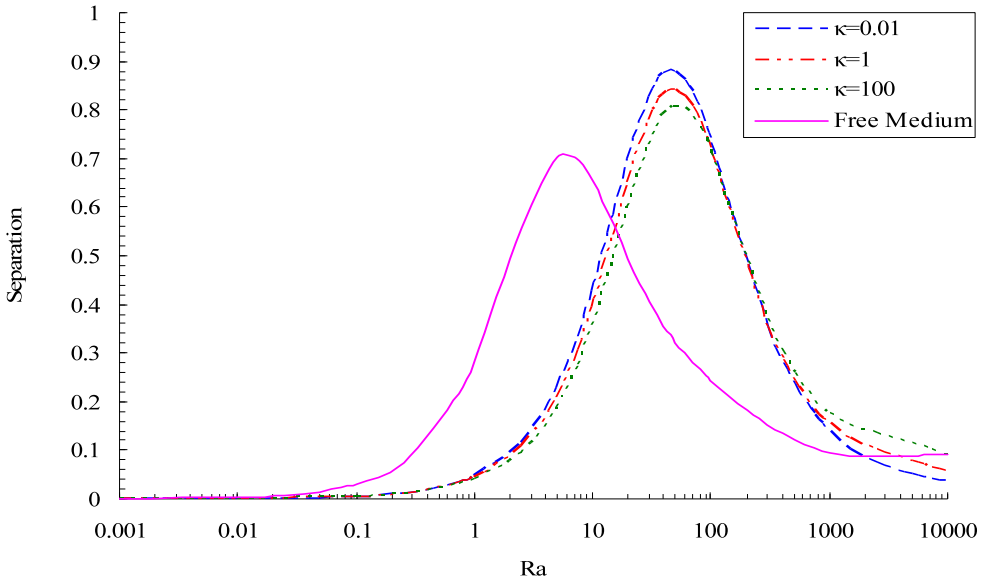

Fig. 2. The influence of the Rayleigh number (Ra) on the separation rate in the thermogravitational cell.

The Rayleigh number $Ra = H^3 g\beta_T \Delta T(\rho c_p)_\beta/\upsilon_\beta k_\beta$, the Prandtl number $Pr = (\rho c_p)_\beta \upsilon_\beta/k_\beta$, the Lewis number $Le = k_\beta/(D_\beta(\rho c_p)_\beta)$, the solutal to thermal buoyancy ratio which includes the thermodiffusion coefficient, $\psi = \frac{\beta_C}{\beta_T}\frac{\Delta c}{\Delta T} = \frac{\beta_C}{\beta_T}\frac{D_{T\beta}}{D_\beta}$, the conductivity ratio $\kappa = k_\sigma/k_\beta$, and $r_{\rho c_p}$ defined as $r_{\rho c_p} = (\rho c_p)_\beta/(\rho c_p)_\sigma$.

In the next section, these dimensionless equations have been solved over the thermogravitational cell shown in Fig. 1, and the obtained results have been discussed.

3. Numerical simulations and results

In this section, we present results for the direct numerical simulation of the coupled flow, heat and mass transfer, presented in Eqs. (13)–(23). The numerical simulations of the problems shown in Fig. 1 have been made using the COMSOL™ Multiphysics finite elements code.

The geometry is a vertical column with two arrays of cylinders presenting the solid phase of the packed thermogravitational column. The aspect ratio has been taken equal to two ($A = H/L = 2$). This aspect ratio and the number of cylinders are chosen to be small to enhance the numerical time and calculation precision.

Simulations have been carried out in the case of a binary fluid mixture with properties such as $Le = 122$, $Pr = 13$, $r_{\rho c_p} = 1$, and $\psi = 0.4$, which are close to values corresponding to classical water–alcohol binary mixtures. The separation (S) is defined as the difference of the mass fractions of the denser species between the two ends (top and bottom) of the cell, in the steady state.

Fig. 2 presents the variation of the separation with Rayleigh number for different thermal conductivity ratios. It can be seen that, in all cases, the separation has a maximum; this maximum corresponds to the optimal coupling between thermodiffusion and convection. Here we can easily find that the maximum separation occurred at $Ra_{opt} = 45$ for all the solid/fluid thermal conductivity contrast. When $Ra < 45$, the convection is weak and separation is mainly due to thermodiffusion and in this case it is smaller than the one obtains by optimal coupling. When $Ra > 45$, the convection is intense and then flow remixes the species of the mixture and consequently, one will obtain a smaller separation. The most important result here is that even if the optimal Rayleigh number remains constant for all thermal conductivity ratios, the separation rate is changed by this ratio. Here, the separation rate increases with decreasing the thermal conductivity ratio.

The optimal Rayleigh number for the same configuration but without any porous medium (free medium – continuous line) is about $Ra_{opt} = 5$ with a separation rate smaller than other cases with solid phase case (no continuous lines). We can therefore conclude that the solid phase present in the thermogravitational column causes increasing of the optimal Rayleigh number and increasing of the separation rate than in thermogravitational columns without porous media.

A comparison of temperature, concentration and velocity fields has been plotted in Fig. 3. According to Figs. 2 and 3, for very small Rayleigh number, the separation rate is equal to zero for both porous medium and free medium cases (there is no vertical separation). As we increase the Rayleigh number, we obtain more separation in free fluid column. Then, for $Ra > 10$ the results show more separation in thermogravitational porous medium cell. Here, the existence of the cylindrical solid structures modifies the dynamic of fluid, decreases convection effect, and consequently increases the separation rate.

In order to better understand the influence of thermal conductivity on the separation rate, we have plotted the changing of the separation rate with thermal conductivity ratio for different Rayleigh number, as shown in Fig. 4.

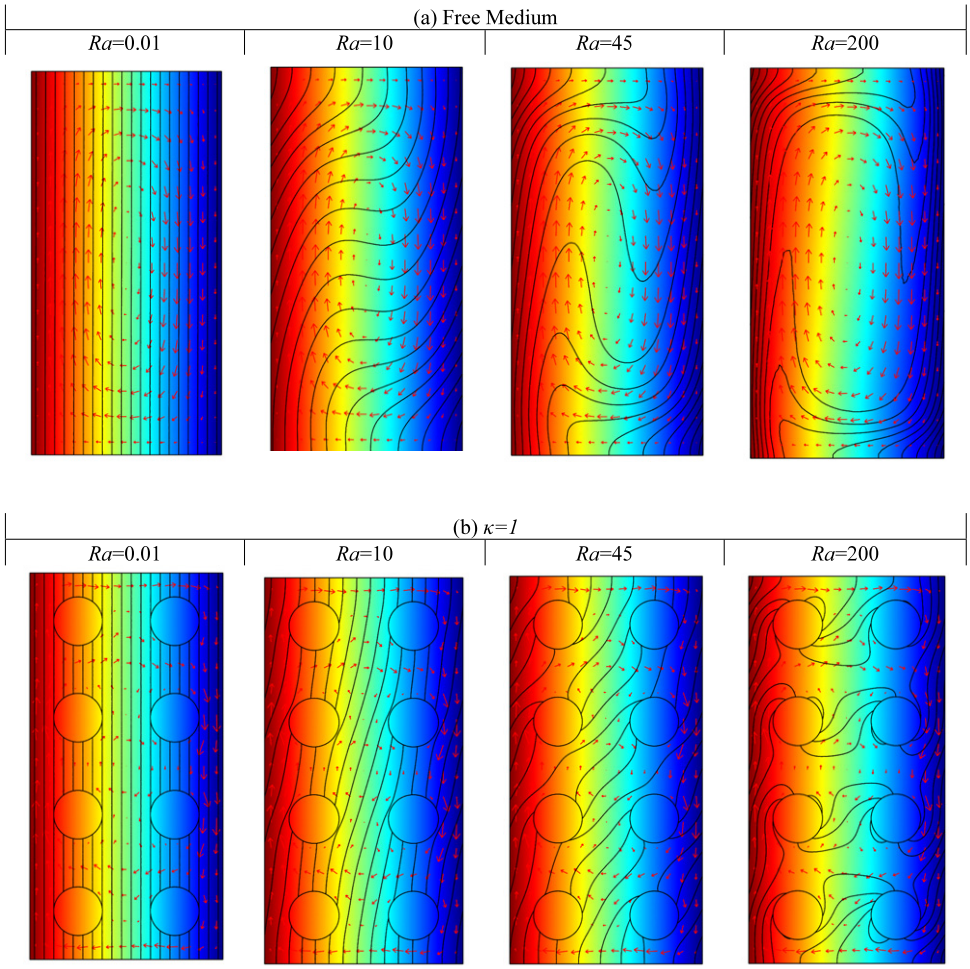

Fig. 3. Temperature (surface), concentration (contour), and velocity (arrow) fields of the cases: a) free medium, b) $\kappa = 1$, and for different Rayleigh number.

As we can see in Fig. 4, for a very small Rayleigh number the separation rate is not dependent upon the thermal conductivity ratio. This result is very similar to the effective thermodiffusion coefficient behavior published recently by Davarzani et al. (2010) [17,18].

For intermediate Rayleigh number the separation rate initially decreases with increasing the thermal conductivity ratio and then reaches an asymptote. As the Rayleigh number increases, convection dominates and the effect of κ on separation rate is completely different. In this case, the separation rate is first increased by κ before reaching the asymptotic behavior.

As we can see in Figs. 2 and 3, between the low and high Rayleigh numbers, there is a transition regime. In this transition regime, there is almost no variation of the separation rate with thermal conductivity ratio.

Fig. 5 shows how thermal properties of the solid structure can change the temperature and concentration distributions at optimal Rayleigh number in a thermogravitational cell.

It can be seen in this figure that when the solid matrix is less conductive than the fluid phase (low κ values), the temperature gradient between the two solid walls in x-direction is less than for other thermal conductivity ratio cases. This causes decreasing the vertical separation resistance and improving the separation rate. Consequently, as the mass transfer is directly related to the thermal distribution, we see that the shape of the iso-concentrations (lines) is different in each case.

4. Conclusion

We have been interested in this study to investigate the influence of the thermal conductivity of the solid matrix in the porous packing of a thermogravitational cell. We used direct numerical simulation to obtain the dynamic, thermal and solutal behavior of both the fluid and the solid in a thermogravitational column made of arrays of cylinders. We have confirmed that the presence of the porous matrix leads to optimal conditions of separation associated to higher Rayleigh numbers than without the porous media. We have also found that taking into account heat transfer in the solid matrix leads to separations greater than the maximum values available in the free case. This is related to the fact that different

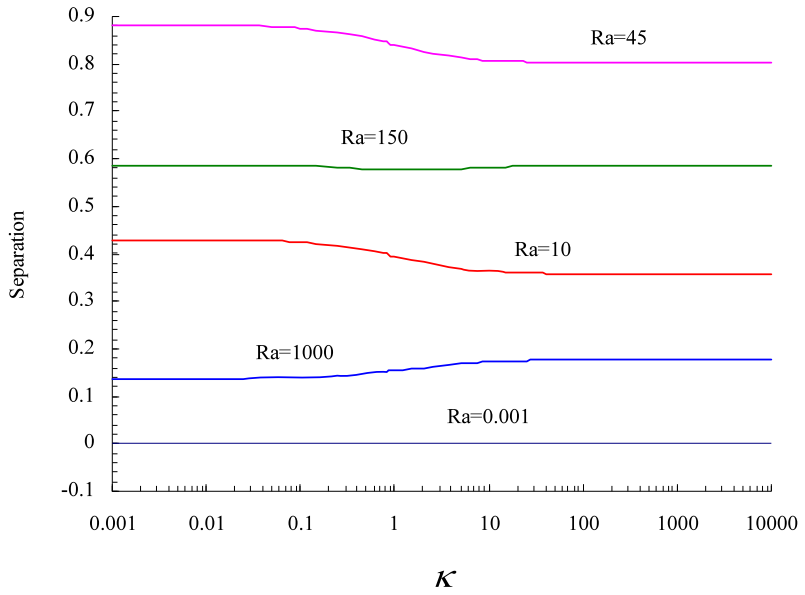

Fig. 4. Influence of thermal conductivity ratio (κ) on the separation rate in the thermogravitational cell.

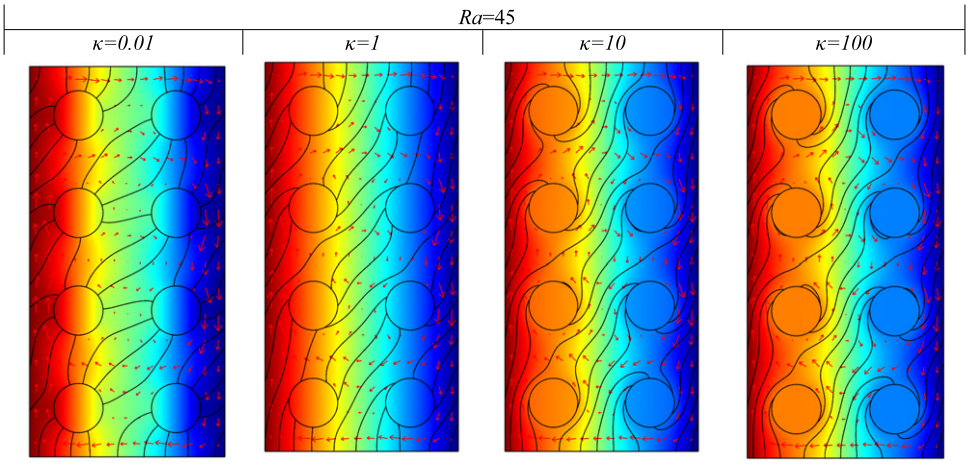

Fig. 5. Temperature (surface), concentration (contour), and velocity (arrow) fields at $Ra_{opt} = 45$, for different thermal conductivity ratios.

conductivity for the solid and the fluid changes the steady state temperature distribution within the cell. Consequently, the concentration field and the separation have been changed by thermal conductivity ratio. In particular, low thermal conductivity of the solid matrix decreases the thermal gradients between the solid walls and improves the separation. This may be one of the reasons of discrepancy which exists between theoretical and experiment results in a packed thermogravitational cell. This may be also a very important starting point to conduct new experimental studies in the future.

Acknowledgements

The authors would like to thank A. Mojtabi and P. Costesèque (Professors at the "Université Paul Sabatier", Toulouse) for valuable comments and helpful discussions.

References

[1] K. Clusius, G. Dickel, The separating tube process for liquids, Naturwissenschaften 27 (1939) 148–149.
[2] W.H. Furry, R.C. Jones, L. Onsager, On the theory of isotope separation by thermal diffusion, Physical Review 55 (1939) 1083–1095.
[3] S.R. De Groot, Phenomenologic theory of the thermogravitational separation mechanism for liquids, Physica 9 (1942) 801–816.
[4] M.M. Bou-Ali, J.J. Valencia, J.A. Madariaga, C. Santamaria, O. Ecenarro, J.F. Dutrieux, Determination of the thermodiffusion coefficient in three binary organic liquid mixtures by the thermogravitational method, Philosophical Magazine 83 (17–18) (2003) 2011–2015.
[5] J.K. Platten, The Soret effect: A review of recent experimental results, Journal of Applied Mechanics 73 (2006) 5–15.

[6] J.K. Platten, P. Costesèque, The Soret coefficient in porous media, Journal of Porous Media 7 (2004) 329–342.
[7] M. Marcoux, P. Costesèque, Study of transversal dimension influence on species separation in thermogravitational diffusion columns, Journal of Non-Equilibrium Thermodynamics 32 (2007) 289–298.
[8] M. Lorenz, A.H. Emery, The packed thermal diffusion column, Chemical Engineering Science 11 (1959) 16–23.
[9] P. Costesèque, M. El Maâtaoui, E. Riviere, Enrichissements sélectif d'hydrocarbures dans les huiles minérales naturelles par diffusion thermogravitationnelle en milieu poreux et cas des isoméres paraffiniques, Entropie 184–185 (1994) 94–100.
[10] M. Marcoux, M.C. Charrier-Mojtabi, Etude paramétrique de la thermogravitation en milieu poreux, Comptes Rendus de l'Académie des Sciences 326 (1998) 539–546.
[11] P. Costesèque, M. El Maâtaoui, Sur la différenciation des hydrocarbures dans les fluids pétroliers par diffusion thermogravitationnelle en milieu poreux en présence d'un contact biphasique huile-eau, Entropie 184–185 (1994) 101–107.
[12] J.K. Platten, Enhanced molecular separation in inclined thermogravitational columns, The Journal of Physical Chemistry B 107 (2003) 11763–11767.
[13] M.C. Charrier-Mojtabi, K. Maliwan, Y. Pedramrazi, G. Bardan, A. Mojtabi, Control of thermoconvective flows by vibration, Mecanique and Industries 4 (2003) 545–549.
[14] B. Elhajjar, M.C. Charrier-Mojtabi, A. Mojtabi, Separation of a binary fluid mixture in a porous horizontal cavity, Physical Review E 77 (1–6) (2008) 026310.
[15] A. Bahloul, M.A. Yahiaoui, P. Vasseur, L. Robillard, Thermogravitational separation in a vertical annular porous layer, International Communications in Heat and Mass Transfer 31 (6) (2004) 783–794.
[16] C.G. Jiang, T.J. Jaber, H. Bataller, M.Z. Saghir, Simulation of Ludwig–Soret effect of a water–ethanol mixture in a cavity filled with aluminum oxide powder under high pressure, International Journal of Thermal Sciences 47 (2008) 126–135.
[17] H. Davarzani, M. Marcoux, M. Quintard, Theoretical predictions of the effective thermodiffusion coefficients in porous media, International Journal of Heat and Mass Transfer 53 (2010) 1514–1528.
[18] H. Davarzani, M. Marcoux, P. Costesèque, M. Quintard, Experimental measurement of the effective diffusion and thermodiffusion coefficients for binary gas mixture in porous media, Chemical Engineering Science 65 (2010) 5092–5104.